J. Fluid Mech. (1982), *vol.* 115, *pp.* 39–58
Printed in Great Britain

The instantaneous structure of mildly curved turbulent boundary layers

By B. R. RAMAPRIAN
Institute of Hydraulic Research, The University of Iowa, Iowa City
AND B. G. SHIVAPRASAD
Department of Civil and Mechanical Engineering,
Southern Methodist University, Dallas, Texas

(Received 18 August 1980 and in revised form 6 April 1981)

Even mild longitudinal wall curvature is known to produce significant effects on the time-averaged turbulent transport in a boundary layer. The present study was undertaken to study the manner in which the instantaneous structure of turbulence in the boundary layer responds to mild streamline curvature. Both convex and concave boundary layers with a boundary-layer thickness to wall radius ratio of about 0·01 were studied. Attention was directed mainly to two events characterizing the instantaneous turbulence structure. These were the so-called 'bursting' and 'zero-crossing'. Quantitative data on the statistics of these events were obtained using a combination of analog instrumentation and visual counting (from continuous film records). These data were compared with data from flat-wall boundary layers obtained from similar signal-processing techniques. The results indicate that neither the individual nor the joint statistics of these events are significantly affected by curvature in the vicinity of the wall. On the other hand, curvature seems to affect appreciably at least some properties of these events at large distances from the wall. Careful examination of these results shows, however, that neither the process of turbulent production near the wall nor the turbulent dissipative process anywhere in the boundary layer is significantly affected by mild curvature. Apparent curvature effects on the instantaneous structure in the outer part of the boundary layer can be explained as being due to the strong effect of streamline curvature on the turbulent diffusion process. This explanation is consistent with previous observations of the time-averaged structure of the flow. The results of the present study indicate the need to re-examine some of the recent turbulence models for curved flows that involve modification of the production and dissipation terms rather than the diffusion term in the transport equations.

1. Introduction

It is now well known (Bradshaw 1969; Shivaprasad & Ramaprian 1978; Ramaprian & Shivaprasad 1978; Meroney & Bradshaw 1975) that even mild streamline curvature has significant effects on the overall behaviour of turbulent shear flows. Specifically, in the case of a boundary layer in zero pressure gradient, convex wall curvature significantly reduces the Reynolds shear stress and the length scale of turbulence while concave curvature has the opposite effect. In an earlier paper (Ramaprian & Shivaprasad 1978), the authors concluded from measurement of triple correlations that the

effect of mild curvature ($|\delta/R_w| = 0{\cdot}01$, where δ is the boundary-layer thickness and R_w is the radius of curvature of the wall) on the turbulent boundary layer is due predominantly to the modification of the diffusion process in the middle part of the boundary layer. It was found, however, that there was very little effect of mild curvature on either the mean flow or turbulent stresses in the near-wall region ($y^+ < 200$). It was also found that mild curvature has negligible effect on the rate of turbulent energy dissipation. In fact, curvature seems to affect predominantly the larger eddies in the turbulent flow. One would thus expect that calculation procedures for turbulent boundary layers on curved surfaces should be sensitive to the diffusion model used and relatively insensitive to the handling of the dissipation process. However, recent reports seem to indicate that such predictions can be improved by modifying the terms associated with production/dissipation processes in the model equations and with no modification of the diffusion term. For example, Launder, Priddin & Sharma (1977) report that good predictions can be obtained by using their k-ϵ model but with curvature correction applied to the sink term in the ϵ-equation. These mutually contradictory results can of course be reconciled by explaining that, after all, the inherently large number of degrees of freedom characteristic of such calculation procedures would allow one to obtain good overall predictions even though individual terms in the governing equations may not be accurately modelled. However, these raise a basic question as to what really is the effect of wall curvature on the detailed structure of turbulence. It would hence be interesting to study how the instantaneous structure of turbulence including the mechanism of the so-called turbulent 'bursting' process in the boundary layer is affected by streamline curvature. Such studies have been made quite extensively in flat-wall boundary layers. These experiments have provided detailed information on aspects such as the frequency and duration of bursting, the zero-crossing frequency of the instantaneous velocity fluctuations and its relation to the Taylor microscale. The present paper reports experimental data on the instantaneous structure of turbulence in boundary layers over mildly curved convex and concave walls and examines these results in the context of the corresponding results for flat-wall boundary layers.

2. Experimental details

2.1. *Experimental conditions*

The measurements reported in this paper were made in the same experimental apparatus as the one used in the studies reported earlier. The apparatus consisted of a curved test section 250 mm high × 100 mm wide. A schematic diagram of the test section is shown in figure 1. The test facility is described briefly in the earlier papers of the authors (Ramaprian & Shivaprasad 1978, Shivaprasad & Ramaprian 1978) and in detail in Ramaprian & Shivaprasad (1976). The convex and concave walls of the test section had radii of 2·490 m and 2·590 m, respectively. The value of δ/R_w for both the walls was approximately 0·013. It was ensured that the boundary layers on the two walls were separated by a core of non-turbulent fluid even at the last measuring station (station 35) along the curved section. All the experiments were carried out under nominally zero-pressure-gradient, two-dimensional conditions. The momentum-thickness Reynolds number R_θ of the flat-wall boundary layer at the inlet to the curved section was about 2400. The free-stream velocity at the inlet to the curved

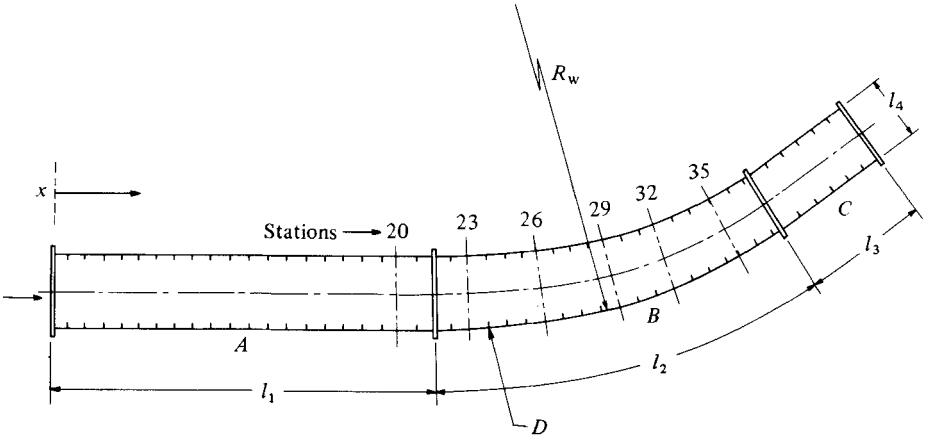

FIGURE 1. Measurement locations and flow conditions. A, inlet straight section; B, curved test section; C, exit straight section; $l_1 = 1{\cdot}28$ m, $l_2 = 1{\cdot}19$ m, $l_3 = 0{\cdot}3$ m, $l_4 = 0{\cdot}10$ m; $R_w = 2{\cdot}49$ m for convex wall and 2·59 m for concave wall.

Wall	Measurement station	x (m)	$\bar{U}_{pw}$ (m/s)	δ (mm)	R_θ (approx.)
Flat	20	1·03	22·1	19·5	2400
Convex	35	2·18	23·4	29·6	4800
Concave	35	2·22	22·5	33·2	5000

section was approximately 22 m/s. Measurements reported in this paper were made at stations 20 (flat-wall boundary layer) and 35 (curved-wall boundary layer) (see figure 1). The boundary-layer properties at the measuring stations are given in the caption to figure 1.

2.2. *Experimental procedure*

The total head in the boundary layer was measured using a round total head tube of 0·8 mm outside diameter. Turbulence measurements were made using dual-channel constant-current hot-wire anemometry and other associated instrumentation. The thermal inertia of the probe was electronically compensated by a carefully designed and tested circuit. The overall frequency response of the system was flat in the range of 4 Hz–8 kHz (99 % of the energy-containing range) and within 3 db in the range 2 Hz–10 kHz. The hot-wire signals were not linearized, but the error due to this is estimated to be unimportant in the flow region measured and for the purpose of the present study. The instantaneous u and v signals from the hot-wire instrumentation were passed through a pair of signal splitters similar to the type described by Wallace, Eckelmann & Brodkey (1972). The splitters gave either the positive or negative part of the input signal (i.e. u_+ or u_- and v_+ or v_-). The split signals were passed through identical low-pass filters set at 10 kHz to remove any undesirable noise. Also the unsplit u-signal was passed through a Krohn–Hite band-pass filter set at a centre frequency of 3 kHz. The band-pass-filtered signal u_p exhibiting intermittent pulse-like (bursting) structure was amplified and half-wave rectified to obtain the positive half u_{p+}. Four-quadrant analog multipliers and a time-averager (with an averaging time of up to 100 s) were used to obtain the required correlations and r.m.s. values. The various signals could also be observed on an oscilloscope and photographed on

continuous 35 mm film using a drum camera. The dual-beam oscilloscope, together with electronic beam switches, could display up to four different events simultaneously. With this system, it was possible to obtain continuous photographic recording of any three signals along with a reference 100 Hz sine wave which served as the time base. The films were used later to study qualitatively the correlation between various events and also for obtaining quantitative estimates of pulsing (bursting) frequency, zero-crossing frequency, etc.

2.3. *Processing of pulses*

It is necessary at this stage to mention something about the procedure used for the processing of the data on instantaneous structure. We use here the same definition for 'pulses' as used by Badri Narayanan, Rajagopalan & Narasimha (1977), namely the intermittent high-frequency activity observed in the band-pass-filtered turbulent signal. It is important to note that these 'pulses' are *not* synonymous with the turbulent 'bursts' usually referred to in the literature, though they may often be closely related to each other. This aspect will be discussed in detail later in this paper. The centre frequency f_0 of the band-pass filter was, as mentioned earlier, 3 kHz and was slightly larger than the peak of the dissipation spectrum in the curved boundary layers. The bandwidth was $0{\cdot}1f_0$. These values were chosen on the basis of previously documented recommendations (Badri Narayanan *et al.* 1977). Sensitivity of the pulse-frequency data to the selection of the centre frequency of the band-pass filter has been a point of some controversy among researchers (see for example Antonia, Danh & Prabhu 1976). It does seem, however, that the dependence of pulse frequency on the filter frequency, even if not completely absent, is considerably reduced at filter frequencies larger than the peak frequency of the dissipation spectrum. Again, the same authors have shown that the results are not sensitive to the choice of bandwidth. The frequency f_p and width W_p of the pulses were measured using the discriminator technique of Rao, Narasimha & Badri Narayanan (1971). These data were obtained from one-minute continuous film records of instantaneous velocity. An enlarged trace of the photographed signal was copied on to a long roll of graph paper, from a micro-film reader. Several hundred feet of such rolls were processed manually to obtain raw information on frequencies and durations. The information was later used with a computer program to generate useful statistical information on the pulses. The present data thus represent a judicious combination of subjective judgement and a consistent and objective evaluation of the statistical properties. In most cases, up to 600 samples were used in these evaluations and the results were found to be statistically very stable.

An important question that needs to be answered at this stage is related to the significance of f_p as measured in the present experiment as well as by many previous investigators. The band-pass-filtered signal represents, of course, the turbulent activity in a fairly high frequency band (beyond much of the energy-containing range) of the turbulent energy spectrum. It is usually assumed (with good supportive evidence) that this high-frequency activity is generated during the process of turbulent energy production and hence should be observed predominantly during periods of significant turbulent production. Thus, if it is further assumed that turbulent production is largely associated with the process of bursting in the vicinity of the wall, one concludes that the frequency of these high-frequency pulses must correspond to the frequency of bursting. In this sense, one should be able to compare f_p with burst frequencies

observed by, say, Kline *et al.* (1967) from hydrogen-bubble techniques. The band-pass-filtered signal can thus be viewed as the signature of the turbulent bursts. Hence, at or in the immediate vicinity of the wall, the value of f_p should closely correspond to the frequency of bursting f_b. However, at large distances from the wall, f_p, *as measured*, will be determined by several factors, such as the burst frequency at the wall, possible (bursty) production locally and the diffusion of turbulence from the wall region. At very large distances from the wall, local production is very small and thus f_p is, at best, a combined measure of the diffusion characteristics in the boundary layer and the process of turbulent-energy production near the wall.

2.4. *An alternative technique for measuring bursting frequency*

There is no doubt that determination of burst (or pulse) characteristics is subject to considerable uncertainty. Most of it is due to the subjectivity involved in the definition and identification of the bursts (or pulses). Several techniques have been used in the past for identifying and counting these structures. These are reviewed in detail by Willmarth (1975) and include, in addition to the method of Rao *et al.* (1971), the use of various criteria such as the short-time variance (Blackwelder & Kaplan 1976), short-time-averaged velocity going below a predetermined level (Willmarth & Lu 1972), the amplitude of product signal uv in the second quadrant exceeding a certain 'hole size' during bursting (Lu & Willmarth 1973), etc. One of the diversions undertaken during the course of the present experiments was the study of yet another criterion for detecting the bursty structures. The method is somewhat related in concept to that of Lu & Willmarth mentioned above; namely that the turbulent bursts are strongly associated with the production of Reynolds shear stress. One can then take advantage of the concept that the high-frequency pulses are signatures of the turbulent-production process and should therefore correlate highly with periods of large negative values of the instantaneous product signal uv (i.e. products in the second and fourth quadrant). The bursty band-passed signal and the product signal uv were separately passed through signal splitters to obtain u_{p+} (the positive part of u_p) and $(uv)_-$ (the negative part of uv), respectively. These two split signals were then multiplied using an analog multiplier. The resulting triple-product signal $u_{p+}(uv)_-$ was indeed found to contain distinctly 'bursty' negative peaks and was photographed on continuous film. It was found that the frequency f_{pr} of occurrence of 'bursts' in this product signal could be counted with very little ambiguity without even any magnification of the filmed record. A sample record of this product signal is shown in figure 2. Some of the characteristics of this frequency will be discussed in § 3.

2.5. *Zero-crossing measurements*

The zero-crossing frequency f_c of the turbulent velocity signal was obtained from the enlarged film records of the split signal u_- (and redundantly from u_+ records) using a sample size of about 600. It may seem, at first sight, that f_c is a less ambiguous quantity to measure, but there was indeed a certain amount of subjectivity in the determination of the 'zero' because of electronic noise and attenuation/amplification of the trace while photographing/reading. More importantly, since the signal was low-pass filtered at 10 kHz, it did not contain the small-scale dissipative eddies. Recent studies by Sreenivasan, Prabhu & Narsimha (1981) seem to indicate that, if all the latter scales

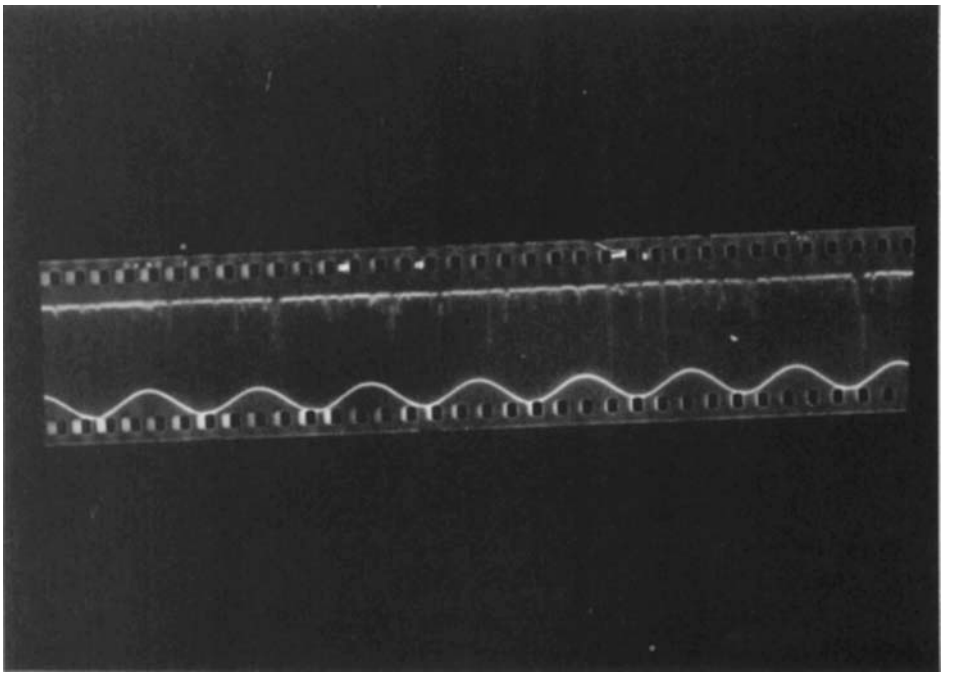

FIGURE 2. Typical photographic record of the trace of the triple product signal $u_{p+}(uv)_-$. The bottom trace is the reference sine wave of 100 Hz.

were contained in the signal, the zero-crossing frequency f_c^* would be much higher than that measured in the present case and would indeed be related to the Taylor microscale λ, via the relation given by Rice (1954), *viz.*

$$\lambda = \frac{\overline{U}}{\pi f_c^*}. \tag{1}$$

The present measurements of f_c can therefore be regarded as the zero-crossing frequency of the energy-containing range of turbulent fluctuations. A length scale $\overline{\Lambda}_u$, defined (following Badri Narayanan *et al.* 1977) as

$$\overline{\Lambda}_u = \frac{\overline{U}}{\pi f_c}, \tag{2}$$

can, therefore, be expected to be larger than λ. This length scale in the present experiments was obtained in basically a similar manner and under similar conditions of Reynolds number, low-pass filtering, etc. to those in the flat-plate experiments of Badri Narayanan *et al.* (though some improvements were made in the processing of data) and hence can be compared directly with the latter for studying curvature effects on the structure of turbulence.

2.6. *Measurement of Taylor microscale*

One often uses the Taylor microscale λ as a reference length scale in the study of the instantaneous structure of turbulence. In the present experiments, λ was obtained from the relation

$$\epsilon = \frac{\overline{u^2}}{\lambda^2}, \tag{3}$$

the dissipation rate ϵ being obtained from the usual approximate relation

$$\epsilon = 15\nu\overline{\left(\frac{\partial u}{\partial x}\right)^2} = 15\frac{\nu}{\overline{U}^2}\overline{\left(\frac{\partial u}{\partial t}\right)^2}, \tag{4}$$

where $\overline{U}$ is the local mean velocity. The dissipation measurements were made with a finer wire (2·5 μm). The differentiation of u with respect to time was performed using an analog differentiator of correct response up to 15 kHz.

Many of the measurements made in the curved boundary layers were also made in the flat-wall boundary layer at station 20. It is, however, the opinion of the authors that some of these data are subjected to considerable uncertainty for several reasons. These are: (i) the boundary-layer thickness at this station was too small (see figure 1) to obtain reliable measurements with an X-probe; (ii) the centre frequency of the filter, *viz.* 3 kHz, while adequate for the curved boundary layers downstream, was probably much smaller than the peak frequency of the dissipation spectrum (about 6 kHz at this station) – unfortunately a late realization ! Hence, these flat-wall data are presented in this report simply for the information of the reader. Results for flat-wall boundary layers from Badri Narayanan *et al.* (1977) (which were obtained at a Reynolds number similar to the present curved-boundary-layer experiments and using similar instrumentation) are used for comparison with the present curved-boundary-layer data.

3. Results and discussion

3.1. *Pulse frequency*

Attempts have often been made in the past to correlate data on the 'bursting' frequency in a boundary layer using the free-stream velocity U_∞ and the boundary-layer thickness δ as the scaling quantities. The result has been assumed to be synonymous with the pulsing frequency f_p of the band-pass-filtered u-signal from the hot wire and measured from the record of the latter signal. Figure 3 shows a plot of $\overline{U}_{pw}/f_p\delta$ versus y/δ from the present experiments. The quantity $\overline{U}_{pw}$ denotes the potential flow velocity at the curved wall and is equal to U_∞ when used with a flat-wall boundary layer. The results of some previous studies are also indicated in the figure. It is easily seen that there is a considerable variation (0·5–4) in the value of $\overline{U}_{pw}/f_p\delta$ obtained by different investigators even for a flat-wall boundary layer. Nevertheless, it is generally accepted that the pulsing (bursting) rate scales with U_∞ and δ over a reasonably large range of Reynolds number and that the value of $U_\infty/f_p\delta$ is in the range of 1·4–2·4 in the vicinity of the wall. It is also believed that this value does not change significantly across a flat-wall boundary layer. The departure from this trend of the present flat-wall boundary-layer data shown in figure 3 is difficult to explain except as being due to the choice of too small a filter frequency (as already discussed).

While considerable variations are apparent between the data of different investigators, it is seen from figure 3 that the present curved-wall data indicate that, near the wall, the non-dimensional pulse rates are almost unaffected by mild wall curvature. The results for convex- and concave-wall boundary layers in the near-wall region are in close agreement among themselves as well as with the flat-wall data of Badri Narayanan *et al.* (1977). In the outer part of the boundary layer, however, one can observe a difference between the two curved boundary layers. The concave-wall data

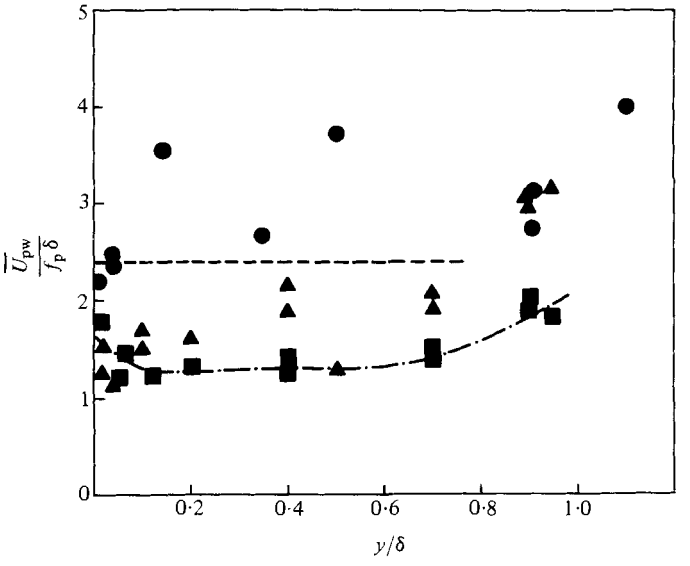

FIGURE 3. Scaling of pulsing frequency in boundary layers. - - - -, flat wall boundary-layer data of Rao *et al.* (1971), at $R_\theta \simeq 600$. — · —, flat-wall boundary-layer data of Badri Narayanan *et al.* (1977) at $R_\theta \simeq 3000$. ●, present flat-wall data ($R_\theta \simeq 2400$); ■, present convex-wall data ($R_\theta \simeq 4808$); ▲, present concave-wall data ($R_\theta \simeq 5000$).

indicate a reduction in the non-dimensional frequency of pulses by a factor of 2 while the convex-wall data show a nearly constant value of pulse frequency across the boundary layer, very similar to the flat-wall data of Badri Narayanan *et al.* Figure 4 shows a dimensional plot of f_p versus distance from the wall for the two curved boundary layers. This plot shows the difference in the structure of two boundary layers which started from identical conditions and developed along nearly the same length of mildly curved walls of equal but opposite curvature. Again, in the immediate vicinity of the wall, say the first few millimetres, there is no significant difference in the pulse frequency over the two walls. In the outer part of the boundary layer (say beyond 7 mm), however, a significant difference is observed.

The results shown in figures 3 and 4 thus indicate that mild curvature of either sign does not significantly affect the mechanics of the bursting process, i.e. eddies of approximately twice the size of the boundary layer participate in the bursting process in both cases. This new observation combined with the fact that there is very little change in the rate of turbulent energy production in the mildly curved boundary layer (see Ramaprian & Shivaprasad 1978) strengthens the belief that one should look somewhere else (other than the production mechanism) for an explanation of the observed spectacular effects of curvature on the distribution of Reynolds shear stress in the outer region of the curved boundary layer. It was speculated in the paper cited above that the explanation probably lies in the effect of curvature on turbulent diffusion. Specifically, it was shown (from measurement of triple products) that turbulent diffusion in the outer layer is increased by concave curvature and decreased by convex curvature.

The observed decrease of f_p in the outer regions of the concave wall does not contradict the above conclusions. Indeed, from the results of the diffusion measurements and

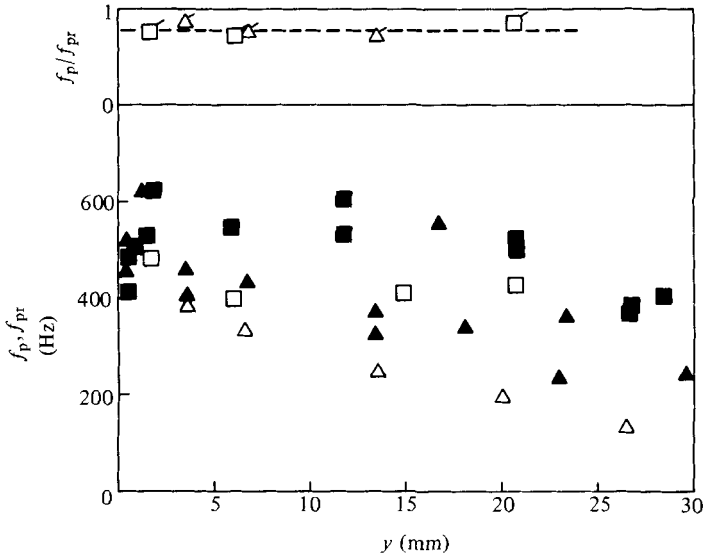

FIGURE 4. Pulse-frequency distribution across the curved boundary layer.

	f_p	f_{pr}	f_p/f_{pr}
Convex	■	□	□
Concave	▲	△	△

with the hypothesis made earlier, namely that f_p as measured in the outer layer is a combined measure of bursting frequency and the diffusion process, a qualitative, but self-consistent, picture emerges. Thus, in the concave boundary layer, increased turbulent diffusion causes some of the burst structure to reach the outer regions and be detected as a pulse. The frequency of this activity decreases as the distance from the wall increases. Again, in the paper cited above, amplitude probability distributions of the turbulent velocity signals were reported. These indicated strong, negatively skewed distributions for the u-signal in the concave boundary layer, suggesting intermittent arrival of fluid from the wall region. Over the convex wall, the outward diffusion is greatly inhibited and thus the observed pulses in the outer region of the boundary layer are predominantly the signatures of the local turbulent production process (however weak it may be) and disappear more or less abruptly at the edge of the boundary layer. Amplitude probability distributions for the convex-wall boundary layer also reported in the above paper showed very little skewing and thus support this statement, at least qualitatively. One would therefore expect to find f_p to be nearly constant across the boundary layer. This expectation, indeed, coincides with the observation.

Figure 4 also shows the distribution across the boundary layer of the frequency f_{pr}, defined earlier. It is seen that these data show very little scatter while still generally agreeing with f_p. The flagged open symbols in figure 4 show the distribution of the ratio f_p/f_{pr} across the boundary layer. The ratio has a constant value of about 0·8 for both boundary layers, showing that a strong correlation exists between the two methods of identifying the fine-scale structure. Apart from being simpler and more objective, the use of f_{pr} instead of f_p as a measure of the intermittency of the high-frequency structure also has the advantage that it reduces the scatter in the data. Further it is weighted

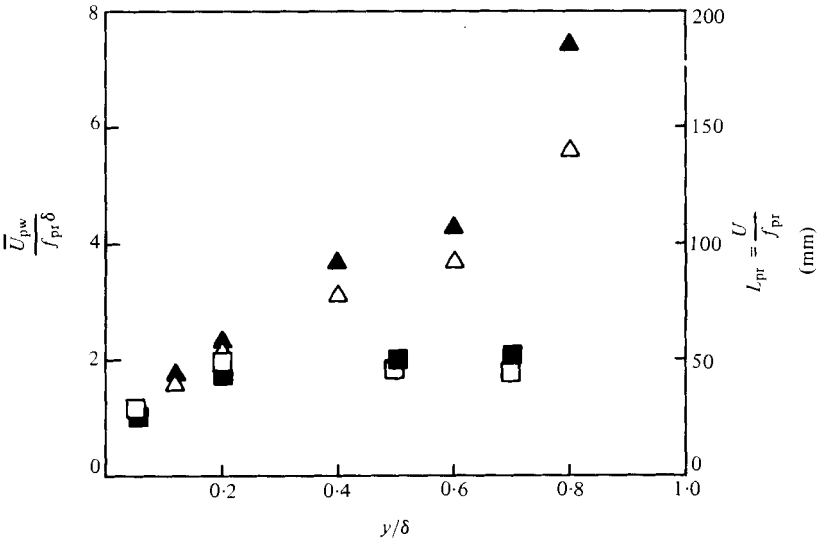

FIGURE 5. Effect of wall curvature on f_{pr} and L_{pr}.

	$U_{pw}/f_{pr}\delta$	L_{pr}
Convex	□	■
Concave	△	▲

with the strength of the production bursts at the wall (via the product uv) and is hence a better measure of the intermittency of the arrival (by diffusion) of fluid from regions of strong turbulent production. Figure 5, which shows plots of $\overline{U}_{pw}/f_{pr}\delta$ and $L_{pr} = \overline{U}/f_{pr}$, is further evidence of the superiority of f_{pr} over f_p as a parameter for the study of the burst production and its diffusion across the boundary layer. Again, from the near-wall data shown in this figure, it is seen clearly that very little effect is produced by mild curvature on the intermittency of the turbulent bursting process.

The quantity L_{pr} can be interpreted as the average spatial interval along the flow between regions rich in small-scale structure. It is seen that L_{pr} is limited to about 1·7 times the boundary-layer thickness in the case of the convex-wall boundary layer while it increases continuously to more than 6 times the boundary-layer thickness in the case of the concave wall. The apparent large effects on f_{pr} and L_{pr} in the outer layer are consistent with the comments made earlier regarding turbulent diffusion.

3.2. *Pulse duration*

In addition to the mean interval $\overline{T}_p(= 1/f_p)$ of high-frequency pulses, the duration W_p of these pulses was also measured (see the definition sketch in figure 6). Since the pulses are representative of the relatively finer structure of turbulence, it is relevant to compare some of their spatial scales with the scale associated with the dissipation process. For example, it is instructive to compare the mean spatial interval $\overline{T}_{sp}$ between pulses and the mean spatial width $\overline{W}_{sp}$ of the pulses (defined by $\overline{T}_{sp} = \overline{U}\,\overline{T}_p$ and $\overline{W}_{sp} = \overline{U}\,\overline{W}_p$, respectively) with the microscale λ. These comparisons are shown in figure 6. The distributions of λ for the two curved boundary layers are also shown in the lower part of figure 6. It is seen that mild curvature has only a small effect on λ, suggesting that the dissipative structure is not significantly influenced by mild stream-

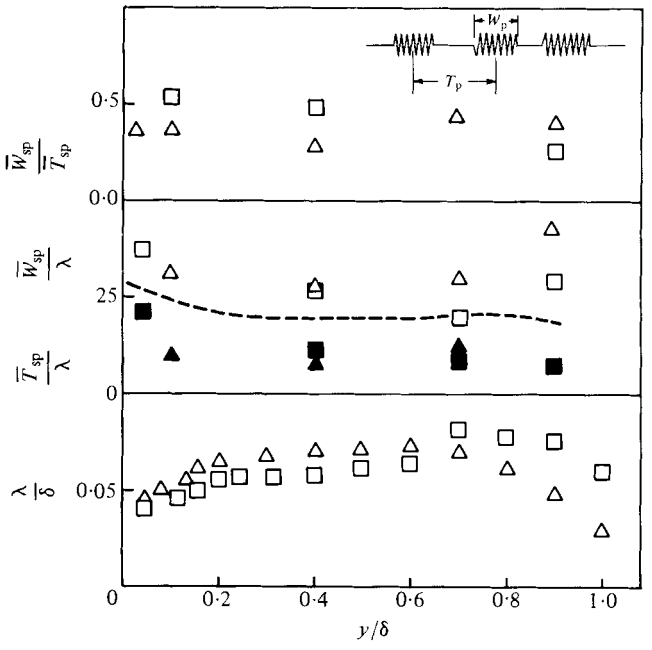

FIGURE 6. The pulse structure in the curved boundary layer and its relation to the Taylor microscale. □, convex wall; △, concave wall. Open symbols in the middle graph denote $\overline{T}_{sp}$ and filled symbols denote $\overline{W}_{sp}$. – – – –, $\overline{W}_{sp}$ data of Badri Narayanan *et al.* (1977).

line curvature. The distributions of $\overline{T}_{sp}/\lambda$ and $\overline{W}_{sp}/\lambda$ are shown respectively by open and filled symbols in the central part of the figure. The $\overline{W}_{sp}$ data of Badri Narayanan *et al.* (1977) for flat-wall boundary layers are also shown by the dotted line. These agree qualitatively with the present results though some quantitative difference is present. The data of $\overline{T}_{sp}$ in regions away from the wall are the result of the combined influence of several factors and are hard to interpret. The present data, however, do show that the spatial interval between high-frequency pulses near the curved walls is of the order of 40λ, which means that the bursting process is triggered by eddies large compared to the microscale and that the dynamics of the bursting process is not significantly affected by mild wall curvature. The average pulse width $\overline{W}_{sp}$ is about 20λ in the immediate vicinity of both the convex and concave walls. It is necessary to caution the reader, however, that the exact value of $\overline{W}_{sp}$ will probably vary with the centre frequency and bandwidth of the filter. The nature of this variation was not investigated in the present case. However, it appears reasonable to conclude that curvature does not significantly affect scales even as large as 20 times the microscale.

Since the band-pass-filtered signal represents the fine-scale structure, one would expect it to exhibit statistical features typical of phenomena dominated by small-scale structures, say dissipative processes. Yaglom (1966) showed that a positive random quantity associated with a dissipative process can be expected to show a log-normal probability-density distribution. The distribution functions for a few quantities associated with flat-wall boundary layers/grid turbulence are shown in figure 7. Kuo & Corrsin (1971) showed that the quantity e^2 (where e is the amplitude of the band-passed signal at a high enough frequency) in isotropic turbulence exhibits a log-normal probability distribution. Their result is shown in figure 7. In this figure $\log_{10}b$ is plotted

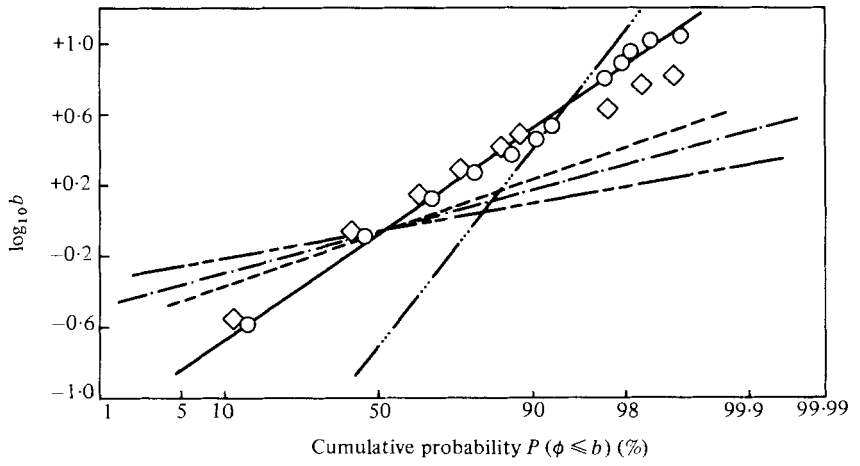

FIGURE 7. Comparison of some of the probability distribution functions associated with the high-frequency pulse structure in turbulent flows.

	Symbol	ϕ	Authors	R_θ	β
Flat-wall boundary-layer results	— — — —	$T_p/\overline{T}_p$	Kim *et al.* (1971)	1100	0·15
	— · — · —	$T_p/\overline{T}_p$	Rao *et al.* (1971)	620	0·155
	— — — —	$W_{sp}/\overline{W}_{sp}$	Badri Narayanan *et al.* (1977)	4200	0·25
	—○—, —◇—	$W_{sp}/\overline{W}_{sp}$	Present data at y = 0·75 mm and 17·78 mm, respectively		0·425
Grid turbulence	— · · · · —	$e^2/\overline{e^2}$	Kuo & Corrsin (1971) (band-pass-filtered signal at 6·3 kHz)		0·91

against cumulative probability P on a probability paper, where P represents the probability that the value of $e^2/\overline{e^2}$ is $\leqslant b$.

Kuo & Corrsin showed that for a log-normal distribution $P_{e^2}(b)$ is given by

$$P = \int_{-\infty}^{\ln b} \left(\frac{1}{2\pi\beta^2}\right)^{\frac{1}{2}} \exp\left[-\frac{(\ln z + \frac{1}{2}\beta^2)^2}{2\beta^2}\right] d(\ln z), \tag{5}$$

where β is the standard deviation of $\ln(e^2/\overline{e^2})$ and is given by the slope of the straight line obtained by plotting $P_{e^2}(b)$ versus $\ln b$ on probability paper. The results of measurements of the distributions of the intervals T_p between pulses, as measured by Rao *et al.* (1971) and of similar intervals between 'bursts', as measured by Kim, Kline & Reynolds (1971) are also shown in the figure. Unfortunately, the interval distribution was not measured in the present experiments. On the other hand, the width distribution of the pulses W_{sp} was measured and is shown in the figure for the flat-plate boundary layer (station 20). Also shown are similar results obtained by Badri Narayanan *et al.* (1977) for a flat-plate boundary layer at R_θ = 3000. It is interesting to compare the various distributions shown in figure 7. To begin with, all these distributions were found to approximate reasonably closely to a log-normal distribution as revealed by data falling on a linear plot on the probability paper. In fact, it is these fitted lines that are shown in the figure. The location of the line depends on the choice of the mean value $\overline{T}_p$ (or $\overline{W}_{sp}$ or $\overline{e^2}$, as the case may be) and is not very significant for the

present discussion. It is important to remember that these distribution curves have all been obtained with a rather limited sample size and hence can only indicate trends. Nevertheless, it is obvious from figure 7 that the $\overline{e^2}$ data of Kuo & Corrsin (1971) show the largest slope (0·91) in comparison with the other data shown in the figure. It can be shown (see Kuo & Corrsin 1971) that smaller slopes indicate larger coherence (or periodicity) while larger slopes indicate larger intermittency. Thus, the amplitude of the filtered signal 'e' of Kuo & Corrsin is more intermittent in the sense that it will be zero during intervals between bursting and non-zero during bursting. The width-distribution data of Badri Narayanan *et al.* on the other hand has a slope of 0·25 and is more coherent. The nearly log-normal distribution of the data shows that the pulses being observed are associated with a process dominated by fine structure. The W_{sp} distribution curve (obtained by a least-square fit of the present data for station 20) for a flat boundary layer also shows a log-normal distribution. It has, however, a somewhat different slope (0·45) from the that of Badri Narayanan *et al.* The reason for this difference is not very clear, particularly since the data for the curved boundary layers shown in figure 8 also exhibit nearly the same slope (0·38). Perhaps the results are sensitive to the particular filter settings and technique used for burst-duration measurement. The probability distributions of T_p obtained by Rao *et al.* (1971) are also seen to follow log-normal distributions but with even smaller slopes ($\simeq 0{\cdot}15$), thereby indicating the existence of an even higher degree of periodicity. The net conclusion that can be generally drawn from figure 7 seems to be that turbulence is generated in bursts near the wall and these bursts can be conceptually regarded as consisting of American-doughnut-shaped vortex structures with an average diameter of $\overline{T}_{sp}$ and an average thickness of $\overline{W}_{sp}$. The size of the doughnut is coherent with a small standard deviation while the thickness is distributed more widely around the average. These observations are consistent with the vortex-tube models proposed recently by several investigators.

Figure 8 shows the duration distribution of pulses for the convex- and concave-wall boundary layers. While the limited sample size (about 600) introduces statistical uncertainties, it is seen that the data for both walls and at all distances from the wall indicate near-log-normal distributions. As already mentioned, the slopes of both distribution curves are about 0·38; which is not too different from the slope obtained for the flat-wall boundary layer in the present experiments. Since the duration distribution of the pulses is determined (obviously) only when pulses are present (unlike the pulse interval, whose values in the outer part of the boundary layer depend not only on the interval of bursting at the wall but on other factors such as the manner in which the bursts diffuse outwards, local production, etc.), it is purely a characteristic feature of turbulence. Figure 8 thus shows that the instantaneous structure of turbulence *produced* in a boundary layer is basically independent of any mild streamline curvature present in the flow.

3.3. *Zero-crossing measurements*

The so-called zero-crossing frequency f_c or the corresponding zero-crossing length scale $\overline{\Lambda}_u$ have often been studied in the past by those doing research on turbulent flows. The present results for f_c and $\overline{\Lambda}_u$ from the study of the curved boundary layers are shown in figure 9. These results can be compared with those of Badri Narayanan *et al.* (1977) for flat-wall boundary layers, shown by dotted lines. It is seen that $\overline{\Lambda}_u/\lambda$ (and

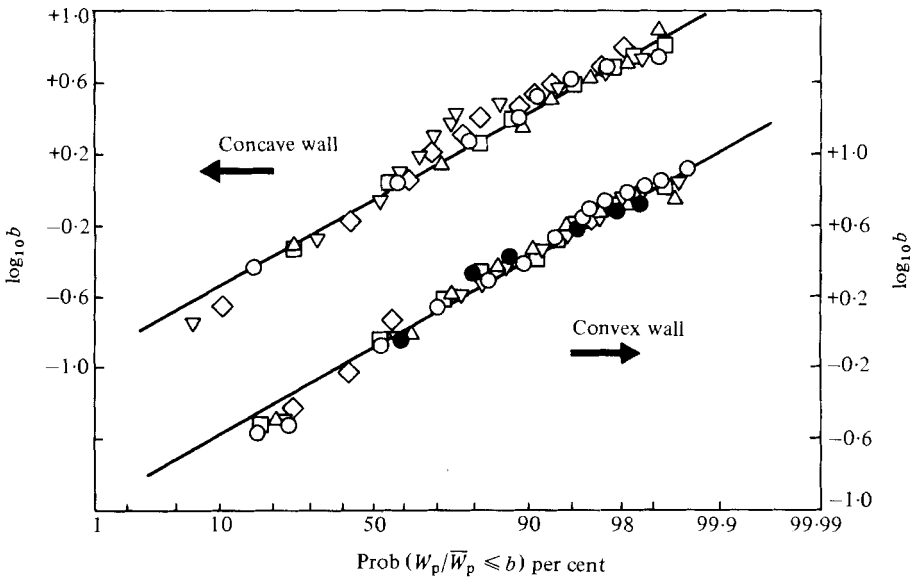

FIGURE 8. Duration distribution of the pulses in the curved boundary layer. Convex wall: □, y = 0·53 mm; ○●, 1·75; ▽, 13·00; △, 22·76; ◇, 29·26. Concave wall: □, $\bar{y}$ = 0·53 mm; ○, 3·94; ▽, 15·13; △, 26·49; ◇, 34·06. The filled circles are data obtained for the negative half of u-pulses. For both walls, the slope β of the fitted straight lines is 0·38.

hence $\bar{\Lambda}_u$) is not significantly affected by curvature *near the wall*. However, it is seen that its distribution in the outer part of the boundary layer is affected by curvature. Specifically, $\bar{\Lambda}_u$ is increased by concave curvature and decreased by convex curvature in this part of the boundary layer, in qualitatively the same way as the length scales L_{pr} or $\bar{T}_{\mathrm{sp}}$ associated with the pulses. The most interesting result, however, seems to be the one shown in the top graph in figure 9. The quantity $2f_{\mathrm{p}}/f_{\mathrm{c}}$, which is the ratio of the pulse frequency to one-half of the zero-crossing frequency, is seen to be of the order of unity for both the boundary layers. This result is in complete agreement with the observations of both Antonia *et al.* (1976) and Badri Narayanan *et al.* The results for a flat-plate boundary layer from Badri Narayanan *et al.* are also shown in the figure.

Since f_{p} and f_{c}, the frequencies associated with the fluctuations, are seen to be very closely related in mean value, one is tempted to compare their statistical properties. One such property, namely the cumulative probability distribution of the length scale Λ_u, is shown in figure 10. Λ_u can be interpreted from (4) to be ($1/\pi$ times) the length of a negative 'run' (i.e. the spatial distance over which *significant* u-velocity fluctuations remain negative at a given instant of time), and can be obtained from a long record of the split u-signal. Badri Narayanan *et al.* (1977) reported that Λ_u is log-normally distributed in the case of a flat-wall boundary layer. The distributions for both convex and concave walls are shown in the figure. These are, however, seen to depart from log-normal distributions. This result is therefore in contradiction of the conclusions of Badri Narayanan *et al.* The authors feel that since Λ_u is not entirely determined by dissipative processes there is no reason to expect Λ_u to follow a log-normal distribution. This is even more so in the outer part of curved boundary layers.

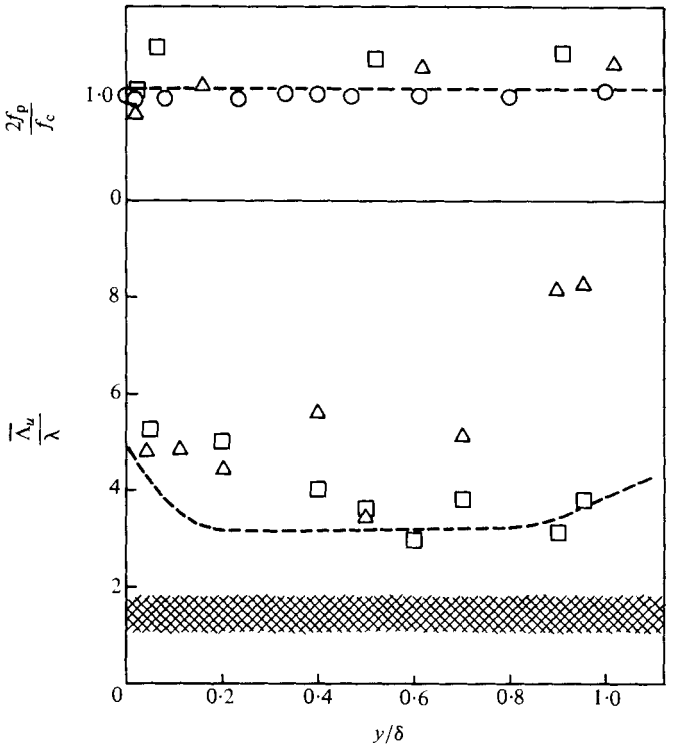

FIGURE 9. The distributions of the zero-crossing length scale and frequency across the boundary layers. □, convex wall; △, concave wall; – – –, $\bar{\Lambda}_u/\lambda$ data of Badri Narayanan *et al.* (1977) at $y/\delta = 0{\cdot}4$; ▨, range of values of $\bar{\Lambda}_u/\lambda$ data of Antonia *et al.* (1976); ---○---, $2f_p/f_c$ data of Badri Narayanan *et al.* (1977) at $y/\delta = 0{\cdot}4$.

3.4. *Joint statistics of pulses and runs*

It will be recalled that $\frac{1}{2}f_c$, as defined in the present study, is the number of intervals ('runs') in a second during which the fluctuations in velocity (of significant energy content) are positive (or negative). The observation that $2f_p/f_c \simeq 1$, which implies that the average pulse interval of the band-pass-filtered signal is nearly equal to the average zero-crossing interval of the low-pass-filtered signal suggests that there may be a direct correlation between the two events; that is, pulses occur largely during a positive-only (or negative-only) velocity fluctuation. Badri Narayanan *et al.* (1977) made some measurements of the coincidence between the pulses and the u_+ and u_- signals. These measurements were made from storage oscilloscope traces and were obtained from a limited sample size. The results indicated that over most part of the boundary layer there was no significant correlation between the pulses and the fluctuations of any one sign. However, very close to the wall ($y^+ < 30$), they observed a strong coincidence between pulses and u_+ fluctuations, while, near the outer edge of the boundary layer, the pulses coincided with u_- fluctuations. These measurements were made in the present studies also but in considerably greater detail. Firstly, the measurements were made from long records which provided a larger sample size (about 600); secondly, the records traced out on large paper rolls allowed the use of a consistent procedure in identifying and counting the pulses and runs; and, finally,

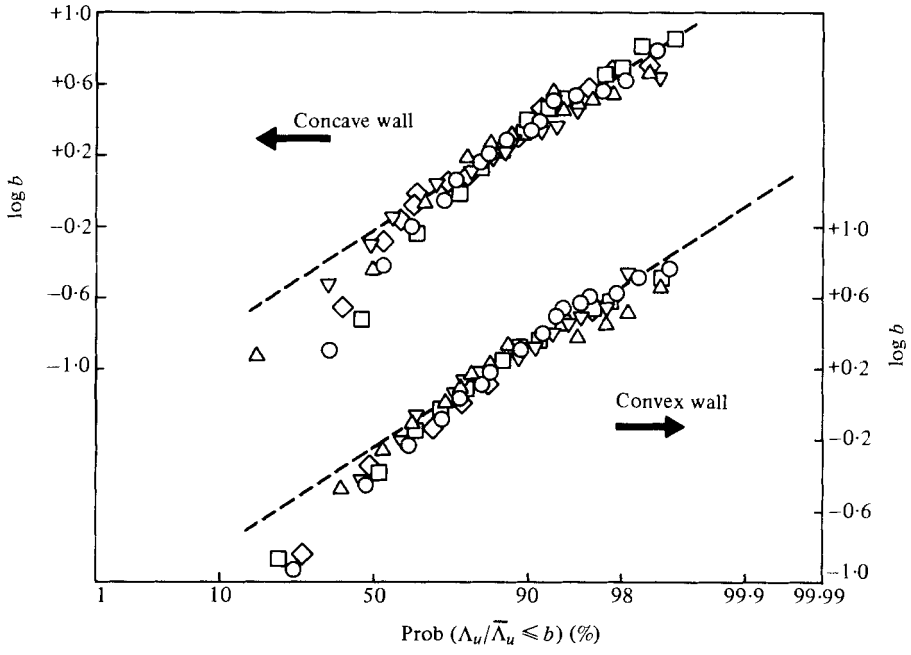

FIGURE 10. Run statistics for u_+ fluctuations (symbols have the same meaning as in figure 8).

a suitably written computer program was used to process the statistics in a well defined manner. In fact, three different types of results were obtained from these studies. These were: the percentage of *number* of pulses that occurred wholly during u_+ and u_- fluctuations; the percentage of the total *duration of pulses* that occurred wholly during the u_+ and u_- fluctuations; a correlation coefficient between these two events, namely pulses and runs. The results for the curved walls are shown in figures 11 and 12. With reference to figure 11, the filled symbols denote percentage of total coincidence between pulses and u_+ fluctuations while the open symbols represent coincidence between pulses and u_- fluctuations. If the two percentages do not add up to 100, it means that there are pulses that overlap across u_+ and u_- fluctuations. It is seen that in both boundary layers, while there is a slight preference (60 % to 40 %) for *more* pulses to occur during u_- fluctuations everywhere in the boundary layer, there is no strong trend indicated, except perhaps near the outer edge. However, if the percentage is based on the duration (width) rather than the number of pulses, stronger trends are indicated, especially for the outer part of the concave-wall boundary layer. It is seen that, especially beyond $y/\delta = 0{\cdot}6$, less than 30 per cent of the duration of pulses coincides with u_+ intervals and the bias toward u_- fluctuations is larger in the outer part of the concave-wall boundary layer than in the outer part of the convex-wall boundary layer. It is, however, seen again that near the wall no significant difference exists between the two boundary layers.

A somewhat more meaningful and quantitative estimate of coincidence is obtained by weighting the events with the amplitude of the fluctuations. This results in arriving at coincidence data between events that contribute significantly to the turbulent activity at a given point. The following procedure was used to quantify the correlation between the pulses and u_+ (or u_-) fluctuations. The filtered u-signal (pulse) was half-

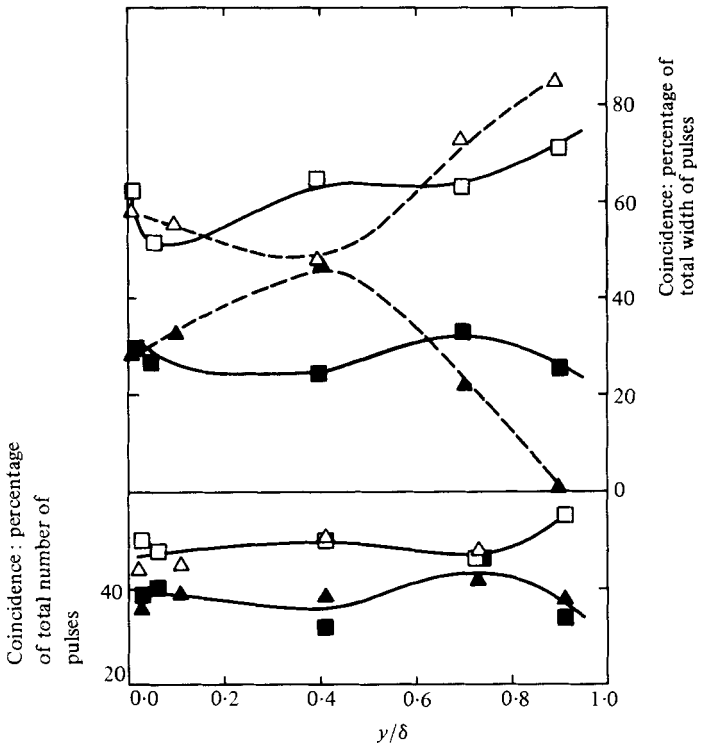

FIGURE 11. Coincidence between pulses and runs. □ ●, convex wall; △▲, concave wall. Open symbols refer to coincidence of u-pulses with u_- fluctuations. Filled symbols refer to coincidence of u-pulses with u_+ fluctuations.

wave rectified and multiplied with the instantaneous split signal u_+ (or u_-). We then define the quantities

$$\left.\begin{aligned} R_{uu_+} &= \frac{\overline{u_+ u_{p_+}}}{(\overline{u_+^2})^{\frac{1}{2}}(\overline{u_p^2})^{\frac{1}{2}}}, \\ R_{uu_-} &= \frac{\overline{u_- u_{p_+}}}{(\overline{u_-^2})^{\frac{1}{2}}(\overline{u_p^2})^{\frac{1}{2}}}, \end{aligned}\right\} \tag{6}$$

where u_p and u_{p+} are the unrectified and rectified filtered signals (pulses), respectively. From the above definition, it is clear that the range of variation of R_{uu_+} is from 0 to 0·5 and that of R_{uu_-} is from 0 to $-0{\cdot}5$. We now define the correlation coefficient C_{uu} as

$$C_{uu} = 2\frac{-R_{uu_-} - R_{uu_+}}{-R_{uu_-} + R_{uu_+}}. \tag{7}$$

From the above definition, it is seen that C_{uu} is a measure of correlation between the u-pulses and u_- fluctuations. C_{uu} will be $+1$ for perfect correlation between u_p and u_- and -1 for perfect anticorrelation between these events (i.e. perfect correlation between u_p and u_+). C_{uu} will be zero if u_p does not correlate with either u_+ or u_-. Figure 12 shows the distribution of C_{uu} for the flat, convex- and concave-wall boundary layers. A small negative correlation is observed between u_p and u_- in the near-wall region – a result in

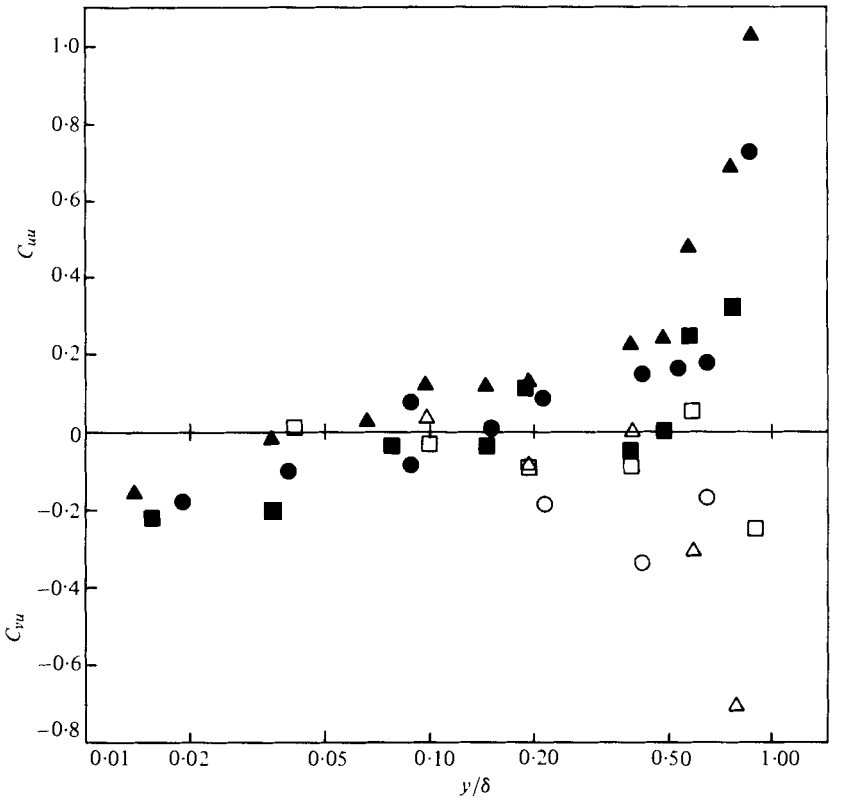

FIGURE 12. Correlation of u_- and v_+ fluctuations with u-pulses. □■, convex wall; △▲, concave wall; ○●, flat wall. Filled symbols refer to correlation with u_- fluctuations and open symbols refer to correlation with v_+ fluctuations.

agreement with the observations of Badri Narayanan *et al.* (1977). However, no great difference is observed between the three boundary-layer data in the near-wall region. In the outer half of the boundary layer, however, it is seen that u_p correlates strongly with u_- fluctuations and the correlation is the strongest in the concave-wall boundary layer and the weakest in the convex-wall boundary layer.

Similar correlation studies were made using the u_p signals along with the v_+ and v_- signals. The resulting correlation coefficient C_{vu} for u_p and v_- signals is defined analogously by

$$C_{vu} = \frac{-R_{uv_-} - R_{uv_+}}{-R_{uv_-} + R_{uv_+}}, \tag{8}$$

where

$$R_{uv_+} = \frac{\overline{v_+ u_{p_+}}}{(\overline{v_+^2})^{\frac{1}{2}}(\overline{u_p^2})^{\frac{1}{2}}}, \quad R_{uv_-} = \frac{\overline{v_- u_{p_+}}}{(\overline{v_-^2})^{\frac{1}{2}}(\overline{u_p^2})^{\frac{1}{2}}}. \tag{9}$$

Since u and v are predominantly anticorrelated one should expect u_p to anticorrelate with v_- in the outer part of the boundary layer. The results are shown in figure 11 and these indicate that C_{vu} increases negatively, approaching -1 in the outer part of the boundary layers. The large u_- or v_+ excursions produced in the outer region of the boundary layer are due to the intermittent arrival of fluid by diffusion from the inner

region. Correlation of pulses with u_- or v_+ fluctuations indicates that these pulses are indeed a part of the local flow structure. Zero-crossing is also clearly a phenomenon strongly related to the arrival of the slow-moving fluid from the wall region. In the outer region of the boundary layer, therefore, one should expect a one-to-one correspondence between the pulse frequency and the zero-crossing frequency, provided that the bulk of the turbulence is received by diffusion from the wall region. This is true even if both these frequencies decrease across the boundary layer from their values at the wall. It is not clear, however, as to why f_p is very nearly equal to $\frac{1}{2}f_c$ in the middle part of the boundary layer where the pulses and runs are not well correlated.

4. Conclusions

The following conclusions can be arrived at from the study reported in this paper.

(1) The instantaneous structure of turbulent production near the wall is not significantly affected by mild longitudinal wall curvature.

(2) Mild wall curvature has very little effect on the fine-scale processes everywhere in the boundary layer. The parameters associated with processes such as the Taylor microscale or the width distribution of the fine-scale structure are not significantly different from those in flat-wall boundary layers.

(3) The instantaneous structure and turbulence statistics associated with it are apparently affected significantly by mild wall curvature in the outer part of the boundary layer. For example, the mean interval between fine-scale structures and the mean zero-crossing frequency of turbulent velocities (both as measured in the present study) are strongly affected by curvature in the outer part of the boundary layer. This apparent effect is believed to be due to the influence of turbulent diffusion, which is known to be very sensitive to streamline curvature.

(4) Notwithstanding the above, the frequency of the high-frequency pulses in the band-passed u-fluctuations is very nearly equal to one-half the zero-crossing frequency of the u-signal (low-pass filtered at the limit of the energy-containing scales) in all cases – a conclusion in agreement with the observations of previous investigators.

(5) The high-frequency u-pulses are well correlated with the negative u-fluctuations (and positive v-fluctuations) near the outer part of the boundary layer. This correlation is the strongest for the concave-wall and the weakest for the convex-wall boundary layer.

(6) The instantaneous product $u_{p+}(uv)_-$ can be used to detect and measure easily the pulse frequency f_p with a relatively high degree of objectivity and consistency.

(7) In the light of conclusions (1)–(3), there is a need to re-examine calculation methods, based on the modification of the production and dissipation models (instead of diffusion models), that claim to predict correctly curved boundary layers, since this approach seems to contradict observations.

REFERENCES

ANTONIA, R. A., DANH, H. Q. & PRABHU, A. 1976 Bursts in turbulent shear flows. *Phys. Fluids* **19**, 1688–1686.

BADRI NARAYANAN, M. A., RAJAGOPALAN, S. & NARASIMHA, R. 1977 Experiments on the fine structure of turbulence. *J. Fluid Mech.* **80**, 237–257.

BLACKWELDER, R. F. & KAPLAN, R. E. 1976 On the wall structure of the turbulent boundary layer. *J. Fluid Mech.* **76**, 89–112.

BRADSHAW, P. 1969 The analogy between streamline curvature and buoyancy in turbulent shear flow. *J. Fluid Mech.* **36**, 177–191.

KIM, H. T., KLINE, S. J. & REYNOLDS, W. C. 1971 The production of turbulence near a smooth wall in a turbulent boundary layer. *J. Fluid Mech.* **50**, 133–160.

KLINE, S. J., REYNOLDS, W. C., SCHRAUB, F. A. & RUNSTADLER, P. W. 1967 The structure of turbulent boundary layers. *J. Fluid Mech.* **30**, 741–773.

KUO, A. Y. S. & CORRSIN, S. 1971 Experiments on internal intermittency and fine-structure distribution functions in fully turbulent fluid. *J. Fluid Mech.* **50**, 285–319.

LAUNDER, B. E., PRIDDIN, C. H. & SHARMA, B. I. 1977 The calculation of turbulent boundary layers on spinning and curved surfaces. *Trans. A.S.M.E.* I, *J. Fluids Engng* **99**, 231–239.

MERONEY, R. N. & BRADSHAW, P. 1975 Turbulent boundary layer growth over a longitudinally curved surface. *A.I.A.A. J.* **13**, 1448–1453.

RAMAPRIAN, B. R. & SHIVAPRASAD, B. G. 1976 An experimental study on the effect of mild longitudinal curvature on the turbulent boundary layer. *Dept of Aeronautical Engineering, Indian Inst. of Science, Bangalore, Rep.* no. 76FM2.

RAMAPRIAN, B. R. & SHIVAPRASAD, B. G. 1978 The structure of turbulent boundary layers along mildly curved surfaces. *J. Fluid Mech.* **85**, 273–303.

RAO, K. N., NARASIMHA, R. & BADRI NARAYANAN, M. A. 1971 The 'bursting' phenomenon in a turbulent boundary layer. *J. Fluid Mech.* **50**, 339–352.

RICE, S. O. 1954 *Selected papers on Noise and Stochastic Processes*, p. 133. Dover.

SHIVAPRASAD, B. G. & RAMAPRIAN, B. R. 1978 Turbulence measurements in boundary layers along mildly curved surfaces. *Trans. A.S.M.E.* I, *J. Fluids Engng* **100**, 37–46.

SREENIVASAN, K. R., PRABHU, A. & NARASIMHA, R. 1981 Zero-crossing in turbulent signals (unpublished manuscript).

WALLACE, J. M., ECKELMANN, H. & BRODKEY, R. S. 1972 The wall region in turbulent shear flow. *J. Fluid Mech.* **54**, 39–48.

WILLMARTH, W. W. 1975 Structure of turbulence in boundary layers. *Adv. Appl. Mech.* **15**, 159–254.

WILLMARTH, W. W. & LU, S. S. 1972 Structure of the Reynolds stress near the wall. *J. Fluid Mech.* **55**, 65–92.

YAGLOM, A. M. 1966 The influence of fluctuations in energy dissipation on the shape of turbulence characteristics in the inertial interval. *Sov. Phys. Dokl.* **11**, 26–29.